Journal of Organometallic Chemistry 693 (2008) 3337–3345

Contents lists available at ScienceDirect

Journal of Organometallic Chemistry

journal homepage: www.elsevier.com/locate/jorganchem

Coupling of Fischer carbene complexes with conjugated enediynes featuring radical traps: Novel structure and reactivity features of chromium complexed arene diradical species

Yi Zhang [a], Tareq Irshaidat [a], Haixia Wang [b], Kris V. Waynant [a], Haobin Wang [a,*,1], James W. Herndon [a,*,2]

[a] Department of Chemistry and Biochemistry, New Mexico State University, MSC 3C, Las Cruces, NM 88003, USA
[b] Department of Chemistry and Biochemistry, University of Maryland, College Park, MD 20742-2021, USA

ARTICLE INFO

Article history:
Received 30 June 2008
Received in revised form 4 August 2008
Accepted 4 August 2008
Available online 12 August 2008

Keywords:
Fischer carbene
Conjugated enediyne
Diradicals
Radical cyclization

ABSTRACT

The reaction of Fischer carbene complexes with conjugated enediynes that feature a pendant alkene group has been examined. The reaction proceeds through carbene–alkyne coupling to generate an enyne–ketene intermediate. This intermediate then undergoes Moore cyclization to generate a chromium complexed arene diradical, which then undergoes cyclization with the pendant alkene group. The radical cyclization prefers the 6-endo mode unless radical-stabilizing groups are present to favor the 5-exo mode. The intermediate diradical species were evaluated computationally in both the singlet and triplet configurations. Arene triplet diradicals feature minimal spin density at oxygen and delocalization to chromium. The 6-endo cyclization product was kinetically and thermodynamically favored.

© 2008 Elsevier B.V. All rights reserved.

1. Introduction

The generation and reactivity of aromatic diradical species emanating from the cyclization of highly conjugated and unsaturated alkyne derivatives has been a very intense area of research since the discovery enediyne anticancer agents [1]. The three major reactions of this type are the Bergman cyclization of conjugated enediynes, the Myers–Saito cyclization of enyne–allenes, and the Moore cyclization of enyne–ketenes, depicted in Scheme 1 (conversion of **B**–**C** in Scheme 1). This paper is focused on the Moore cyclization [2].

The Moore cyclization is limited by the paucity of reaction processes that generate enyne ketene intermediates. The most common process involves thermolysis of 4-alkynyl-2-cyclobutenones (**A**). Alternative but less-commonly employed methods include thermolysis of appropriate α-diazo ketones [3] or thermolysis of appropriate azidobenzoquinones [4], and ene reactions of ethoxyenediynes [5]. A potentially excellent source of enyne–ketenes is the coupling of Fischer carbene complexes (**E**) with readily-available conjugated enediynes (**D**) [6]. Coupling of Fischer carbene complexes with enediyne **D** should proceed through carbene alkyne coupling at the less hindered alkyne unit followed by CO insertion to produce the chromium-complexed enyne ketene species **G** [7], which can then undergo the Moore cyclization to afford arene-complexed diradical species **H** [8]. An alternative method for successful generation of related chromium-complexed arene diradicals involves the coupling of amino-alkynylcarbene complexes with alkynes [9]. In this case the diradical species were successfully quenched with hydrogen atom donors. The trapping of the diradical species through intramolecular hydrogen atom abstraction processes and a single example of trapping through a 5-exo radical cyclization event have previously been reported [8]. In this paper additional examples of the alkene radical trapping reaction and an important structural correction are reported, which reveal interesting and unique features for diradicals generated in the coordination sphere of chromium.

2. Results and discussion

2.1. Experimental results

General synthetic approaches to the conjugated enediynes employed in this study are depicted in Scheme 2. The key step in this process is selective halogen metal exchange in tribromodiene **2** [8], easily obtained through Wittig reaction of the bromo-aldehyde **1** [10]. This process is selective for conversion of the *gem* dibromoalkene group to the enyne-bromide. Subsequent Sonogashira coupling, Swern oxidation and Wittig reaction affords the enediynes used in this study.

* Corresponding authors. Fax: +1 5056462649.
E-mail addresses: haobin@nmsu.edu (H. Wang), jherndon@nmsu.edu (J.W. Herndon).
[1] Computational studies at New Mexico State University.
[2] Experimental studies at New Mexico State University.

0022-328X/$ - see front matter © 2008 Elsevier B.V. All rights reserved.
doi:10.1016/j.jorganchem.2008.08.003

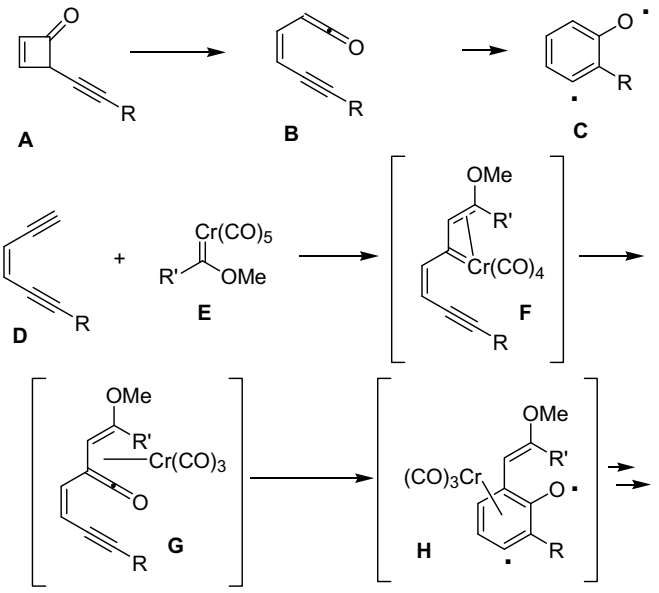

Scheme 1.

In the original report of this reaction (Scheme 3) [8] involving the coupling of enediyne **6a** with Fischer carbene complex **7a** followed by acid treatment, the structures were assigned to the products based on the isolation and full characterization (^{1}H NMR, broad band-decoupled ^{13}C NMR, IR, EI-MS, HRMS) for the major product **13a** and GC–MS and ^{1}H NMR analysis of the crude reaction mixture for the assignment of **14a** and **15a**. The reaction initially afforded enol ethers **9a–12a**, which cyclized to afford the furan derivatives upon acid treatment. As more examples of this type of reaction were acquired, it became apparent that the structure of the major product **13a** was likely misassigned. The isomeric unconjugated dihydronaphthalene structure **16a** was determined to be a better structural fit to the major isomer [11]. Compound **16a** results from a 6-endo radical cyclization rather than a 5-exo radical cyclization (see Section 2.2). The most important evidence is the DEPT C-13 spectrum, which shows that none of the sp^2 carbons are CH_2 groups, and three are CH groups. Another important finding since the original report is that the yield of **16a** relative to the naphthalene structure **15a** is highly variable between experimental runs. Longer reflux times lead to increased amounts of **15a**, which suggests that excessive reflux time causes a slow dehydrogenation of intermediate **12a** to **11a** [12].

The reaction of analogous carbene complexes and enediynes where the trapping alkene group is more substituted are depicted in Table 1. In all of the examples in Table 1, separation of **15** and **16** proved to be very difficult, and the ratio of **15:16** was not constant. Treatment of enediyne **6b** with methylcarbene complex **7a** led to the dihydronaphthalene derivative **16b** accompanied by minor amounts of **15b**. In this case no structural ambiguity exists for **13b** since the methyl group originating at the trapping alkene (δ1.22, doublet, J = 6.0 Hz in the product **16b**) and the alkene protons (δ5.97, broad singlet integrating for 2 H's in product **16b**) are clearly consistent only with **16b**. The use of chlorobenzene as solvent led to a slight improvement in the yield of **16b**. Chlorobenzene is a much poorer hydrogen atom donor compared to dioxane, however is not the optimal solvent for carbene-terminal alkyne coupling reactions that require CO insertion [13]. A similar reaction

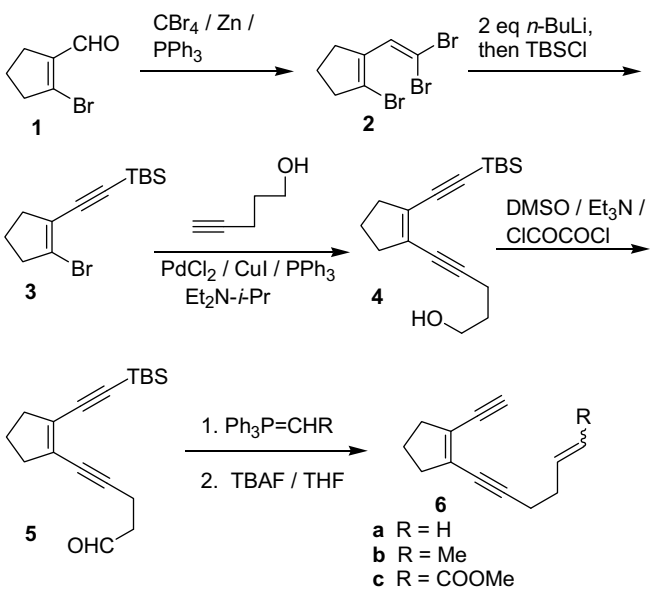

Scheme 2.

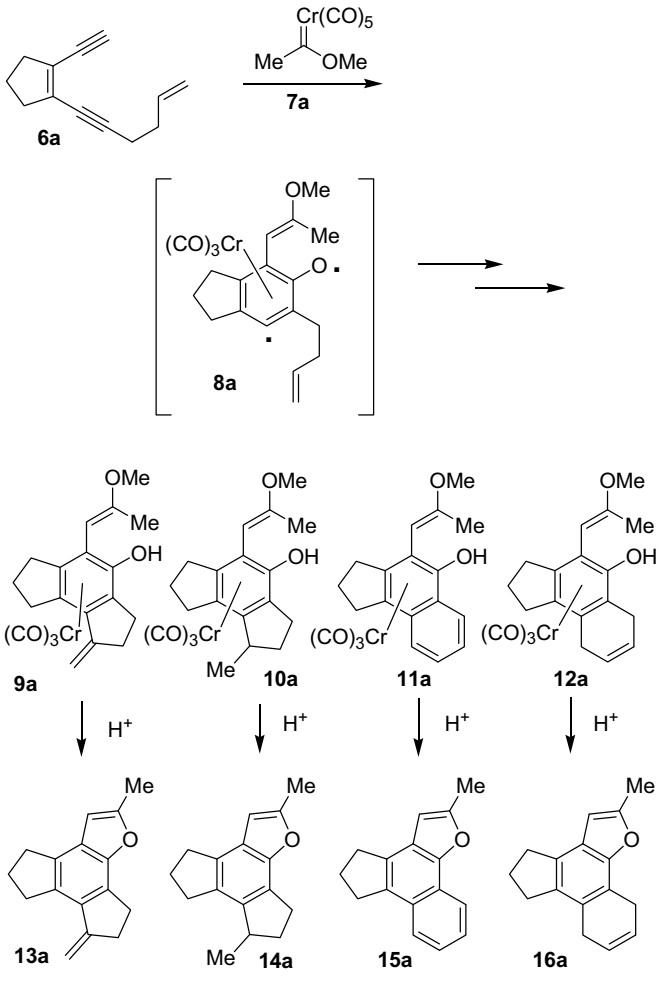

Reported in *J. Org. Chem.* **1998**, *63*, 4562-4563:
13a - 54%, **14a** - 13%, **15a** - 4%, **16a** - not formed

Should be amended to:
13a - not formed, **14a** - < 5% **15a** - highly variable yield, **16a** - major product in 30-54% yield

Scheme 3.

Table 1
Coupling of diene–diynes with Fischer carbene complexes

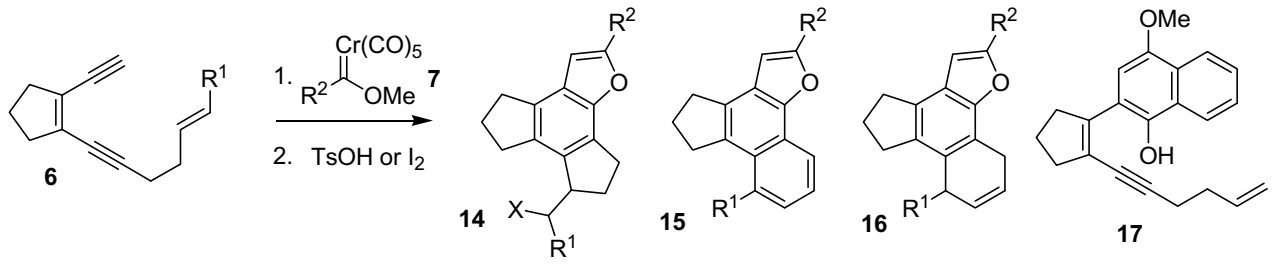

Entry[a]	Reactants	R^1	R^2	X	Solvent	Yield **14**(%)	Yield **15**[b] (%)	Yield **16**[b] (%)
1 (a-series)	**6a + 7a**	H	Me	N/A	Dioxane	Trace	14[c]	54[c]
2 (b-series)	**6b + 7a**	Me	Me	N/A	Dioxane		13	40
3 (b-series)	**6b + 7a**	Me	Me	N/A	Ph–Cl		4	45
4 (c-series)	**6b + 7b**	Me	Ph	N/A	Ph–Cl		Trace	45
5 (c-series)	**6b + 7b**	Me	Ph	N/A	Benzene		21	0
6 (d-series)	**6c + 7a**	COOMe	Me	H	Dioxane	48	0	0

[a] Substituent identifiers for adduct compounds **9–17** and reactive intermediates **18–21** correlate with series letters adjacent to Entry numbers.
[b] The yield of **15** and **16** refers to the isolation of a single chromatography fraction containing both **15** and **16**; the relative proportion was determined through the ^{1}H NMR spectra.
[c] Yield varies widely in experimental runs, however total yield of **15a** + **16a** is consistently about 60%.

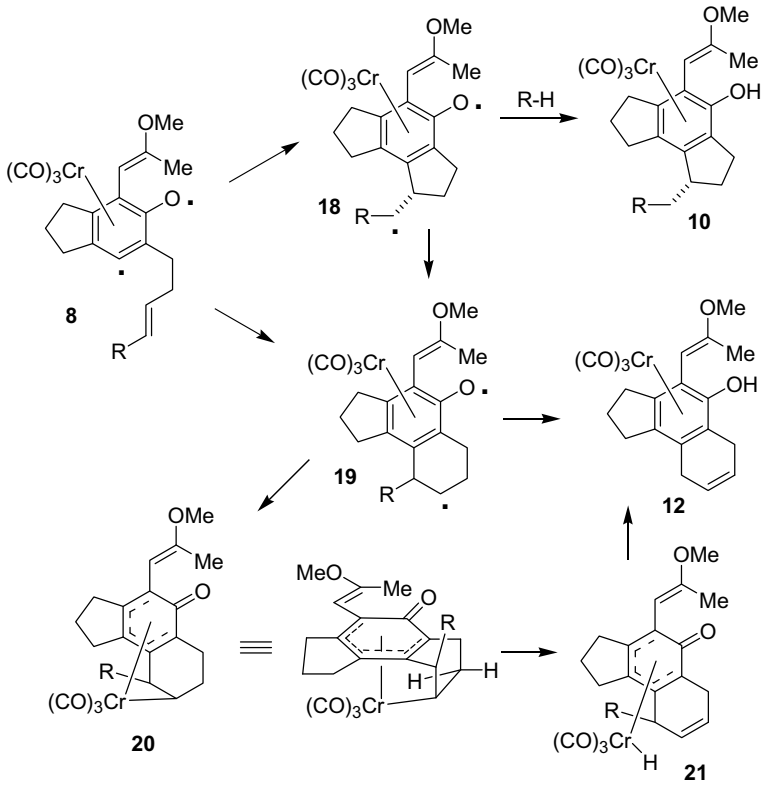

Scheme 4.

process occurred using the phenylcarbene complex **7b**. A noteworthy observation in this reaction is that no product consistent with the Dötz reaction product **17** could be isolated from this reaction. This same reaction in benzene led to the surprisingly selective formation of the naphthalene derivative **15c**, however in low yield. A similar type of reaction was examined using electron-deficient alkenes as the radical trap (entry 6). In these cases, the exclusive reaction products are in fact the reduced 5-exo cyclization product **14d**.

2.2. Discussion of experimental results

A reasonable mechanism for the formation of the observed products is depicted in Scheme 4. After formation of diradical intermediate **8** via the Moore cyclization, radical cyclization can occur in either the 5-exo or the 6-endo mode. Cyclization in the 5-exo mode affords intermediate **10**, the precursor to benzofuran derivative **14**, after transfer of two hydrogen atoms from the solvent. Radical cyclization in the 5-exo mode is typically favored

for arene radicals [14] and for arene-complexed monoradicals [15]. We are not aware of efforts to trap Moore cyclization-derived diradicals through radical cyclization, however they have been trapped through intramolecular hydrogen atom abstraction [4,16]. Successful trapping of related Bergman cyclization and Myers cyclization derived diradicals through 5-exo cyclization has also been reported, however in most of these cases the trapping alkene is a conjugated ester, and reduced products analogous to **14** are typically formed when these reactions are performed in the presence of hydrogen atom donors [17]. In simple radical cyclization reactions, the observation of 6-endo products has typically been attributed to 5-exo-cyclization followed by the neophyll rearrangement process [18]. A similar pathway involving the 6-endo radical cyclization pathway leads to intermediate **12**, the precursor to compounds **15** and **16**. The 5-exo-derived diradical intermediate **18** undergoes hydrogen abstraction, while the 6-endo-derived intermediate **19** undergoes internal hydrogen transfer. A likely explanation for the diverging pathway is due to interaction of the radical species with chromium in intermediate **19**. No such interaction exists for intermediate **18** due to the anticipated stereoselectivity, which places the chromium tricarbonyl unit and the radical substituent on opposite faces of the molecule due to steric interaction between the chromium tricarbonyl and the –CHR· groups [19]. In intermediate **19**, interaction of the radical centers would result in 18-electron complex **20**. Formation of compound **12** from intermediate **20** can be viewed as a β-hydride elimination leading to intermediate **21** followed by reductive elimination and enolization. This process would result in the observed non-conjugated double bond isomer since this isomer arises from the only β-hydrogen syn to chromium in **20**. Significant amounts of the reduced 5-exo product **14** were observed only in the case where R is the electron-withdrawing and radical-stabilizing group COOMe. This is likely due to the stabilization of the 5-exo cyclization derived radical by the COOMe group.

2.3. Results and discussion (computational)

The processes depicted in Scheme 4 were evaluated computationally to gain insight into the rationale for the observed reaction pathways and to better understand the role of chromium in the stabilization and reactivity of diradical intermediates. The reaction pathway under investigation involves the transformation of enyne–ketene complex **22** (Scheme 5) into cyclized diradicals (**24** and **25**). Optimized structures for reactive intermediates **22–25** are depicted in Fig. 1. Theoretical and experimental investigations of arene–chromium complexes that contain a mono-radical at the benzylic and homobenzylic positions have been reported [20]. This study suggested that arene complexation has no major effect on the stability of homobenzylic monoradicals. Hypothetical radical intermediates **18–19** and **24–25** are in fact arene complexed homobenzylic radicals, however these compounds contain a second unpaired electron.

Density function theory (DFT) was used to investigate the intermediates **22–25** and their respective transition states. All calculations were performed with the quantum chemical program package Gaussian 03 [21]. The B3LYP hybrid functional, which includes the Becke three-parameter exchange [22] and the Lee, Yang, and Parr correction functionals [23], was used in the DFT calculation. The SDD [24] basis set was employed for chromium whereas the standard 6-31G* basis set was used for all other atoms. All of the diradical species were evaluated as both singlet and triplet diradicals, and in some cases higher spin configurations were also considered. The resulting conformations and their respective energies are depicted in Fig. 1 and Table 2. The reaction processes are displayed on a potential energy diagram in Schemes 6 and 7. Selected spin densities and bond lengths are depicted in Table 3.

The enyne–ketene complex **22** exists as a diamagnetic low spin complex, which fits related experimental observations where NMR spectra are routinely acquired for various polyene species coordinated to the $Cr(CO)_3$ metal–ligand system. The alkyne group is tilted toward chromium (C5-6-7 angle = 161°, see Fig. 1 for atom numbers), possibly due to the 16-electron configuration at chromium. Higher spin analogues of the enyne–ketene complex **22** were also evaluated. Both the triplet state (+11.4 kcal/mol relative to singlet) and quintet state (+23.3 kcal/mol relative to singlet) were evaluated. In both of these higher spin configurations the spin is concentrated at the chromium atom and not delocalized to any atoms of the polyene ligand.

The initially-formed arene diradical **23** can exist in either the singlet or triplet configuration, depending on whether the individual radical species are spin-paired (singlet) or possess the same spin orientation (triplet). The triplet configuration is more stable than the singlet configuration by 8.5 kcal/mol, however the singlet configuration is presumably the species initially produced from singlet enyne–ketene complex **22**. The spin density of the triplet diradical exists predominantly at chromium and the aromatic carbon designated as C6. Virtually none of the spin density resides at the phenolic oxygen (O1), which is in contrast to the phenoxy radical. The C6–Cr bond distance is considerably shorter in the singlet diradical (1.89 Å) compared to the triplet diradical (2.23 Å). The C–C bond angles at C6 are also different in the singlet (C5-6-7 angle = 133.4°) and triplet (C5-6-7 angle = 127.5°) configurations.

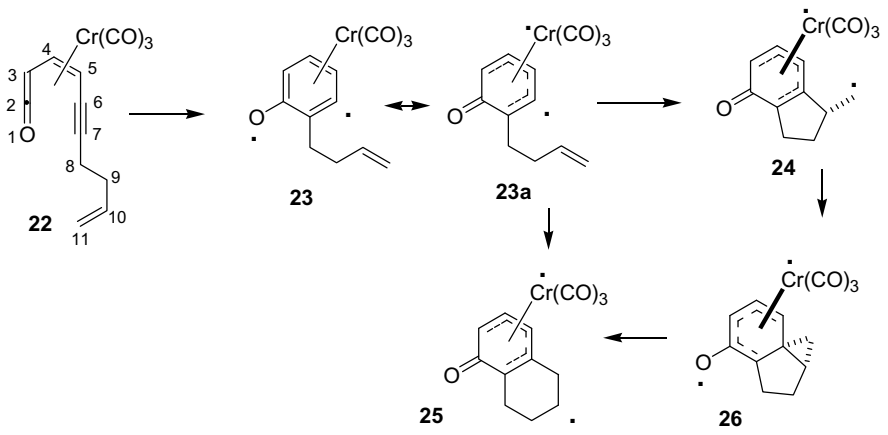

Scheme 5.

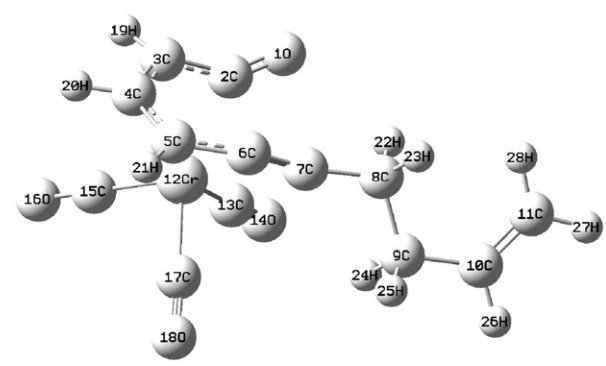

Compound **22**

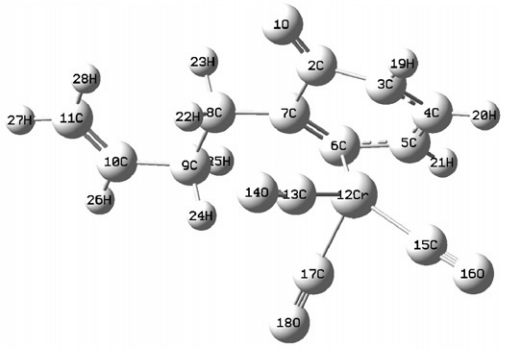

Compound **23a-s**

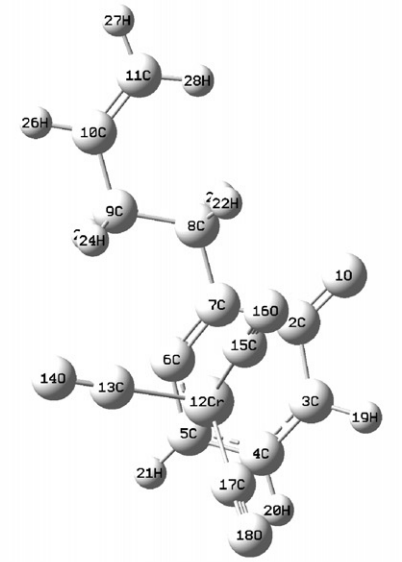

Compound **23a-t**

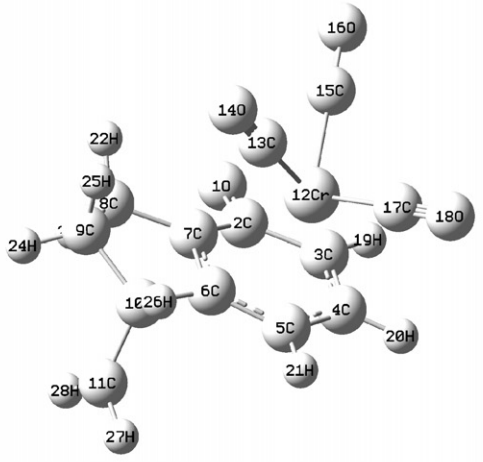

Compound **24-t**

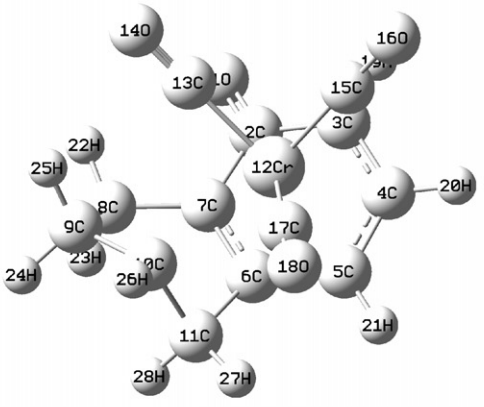

Compound **25-s**

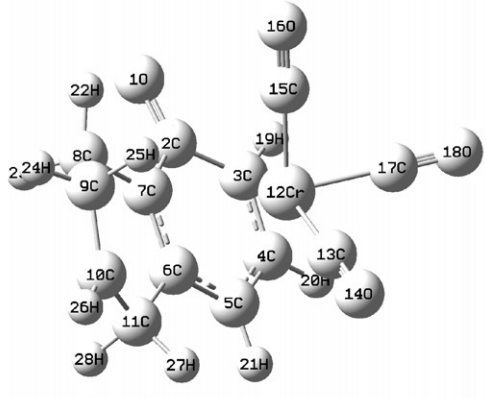

Compound **25-t**

Fig. 1. Energy-minimized conformations of key reactive intermediates.

Intermediate diradical **23** is best represented as the η^5-cyclohexadienyl-Cr(I) resonance form **23a** rather than the η^6-arene complex, regardless of the spin orientation of the radical species. This is also the more appropriate description for related diradicals **24** and **25**. In **23–25** (all spin configurations) the C2–Cr distance is considerably longer that the C–Cr distance for all of the other aromatic ring carbons. The O1–C2 bond length of **23a** (1.22 Å in the singlet, 1.23 Å in the triplet) is indicative of substantial double bond character [25]. By comparison, the corresponding calculated C–O bond lengths are considerable longer in the optimized structures for phenol (1.42 Å) and the simple phenoxy radical (1.30 Å), compared with 1.24–1.27 Å in stable phenoxy radicals [26]. In the simple phenoxy radical the spin density is also concentrated at oxygen (0.51).

Table 2
Relative energies (kcal/mol) for intermediates **22**–**25** and key transition states

Relative energies – G (H)		TS's $\Delta G^{\neq}$ ($\Delta H^{\neq}$)
22	0 (0)	**22** to **23a-s** 9.6 (8.5)
23a-s	+0.7 (−1.1)	**23a-s** to **25-s** 5.2 (3.1)
23a-t	−7.8 (−8.0)	**23a-t** to **24-t** 5.4 (3.2)
24-t	−31.6 (−33.9)	**23a-t** to **25-t** 3.6 (1.2)
25-s	−37.2 (−43.9)	
25-t	−38.7 (−41.1)	

The 5-exo cyclization product **24** was successfully optimized only in the triplet configuration. All attempts to optimize the 5-exo cyclization product in the singlet configuration led to the 6-endo cyclization product **25-s**. Intermediate species during the progression of the optimization of **24-s** bear resemblance to the structure **26** depicted in Scheme 5. The triplet diradical **24-t** prefers the exo configuration of the RCH_2^- group relative to the $Cr(CO)_3$ unit. The spin density is concentrated at chromium and at C11.

The 6-endo radical cyclization product **25** was successfully optimized in both the singlet and triplet configurations, which are very similar in energy (ΔG singlet → triplet = −1.5 kcal/mol). The singlet configuration features a very close contact between chromium and the radical site C10 (2.43 Å), which thus supports the intermediacy of compound **20** in Scheme 4. Bond lengths for chromium bound to sp^3 carbons obtained from X-ray structures vary from 2.26 to 2.34 Å [27]. The spin density in the triplet diradical **25-t** is concentrated at the radical site C10 and at chromium. The 6-endo radical cyclization product **25-t** is substantially more stable than the 5-exo cyclization product **24-t** (ΔG = −7.1 kcal/mol for **24-t** to **25-t**).

The hypothetical reaction pathways, including transition states for all singlet–singlet and triplet–triplet interconversions, are depicted in the potential energy diagrams in Schemes 6 and 7. The pathway through singlet intermediates is depicted in Scheme 6. The Moore cyclization event (conversion of ketene complex **22** to arene diradical complex **23a**) occurs with an activation free energy of +9.6 kcal/mol. Transition state calculations were conducted only for the conversion of **22** to the singlet form of **23a** since **22** is a singlet species. The reaction pathway involving the singlet diradical species can result only in the 6-endo product due to the facile conversion of the 5-exo product to the 6-endo product through an energy barrier lower than that required to recognize a local minimum in a geometry optimization. If the reaction pathway proceeds exclusively through spin-paired diradicals, the 6-endo pathway is the only allowed reaction pathway, regardless of kinetic preferences in the radical cyclization mode. This process is highly exergonic (ΔG = −37.9 kcal/mol) and occurs with a free energy of activation of 5.2 kcal/mol.

The pathway employing triplet intermediates is depicted in Scheme 7. Intersystem crossing from initially-formed intermediate **23a-s** leads to **23a-t** in a process that is exergonic (ΔG = −8.5 kcal/mol). The initially-formed radical can react at the pendant alkene through either the 5-exo mode to afford intermediate diradical **24-t** or through the 6-endo reaction mode to afford diradical **25-t**. Both of the hypothetical reaction products and transition states were optimized. The 5-exo trig cyclization event is highly exergonic (ΔG = −23.8 kcal/mol) and occurs at a moderate free energy of activation (5.4 kcal/mol). The 6-endo trig cyclization occurs with a similar activation energy ($\Delta G^{\neq}$ = 3.6) however results in the thermodynamically more stable product (ΔG = −30.9 kcal/mol for conversion of **23a-t** to **25-t**). If the triplet reaction pathway is preferred the 6-endo and 5-exo radical cyclization pathways are expected to be competitive. The 6-endo pathway is slightly preferred kinetically and strongly preferred thermodynamically.

In summary, the calculations predict that: (1) a reaction that proceeds through the singlet diradical intermediates should result in 6-endo cyclization derived products, and (2) a reaction that proceeds through triplet diradical intermediates could lead to either

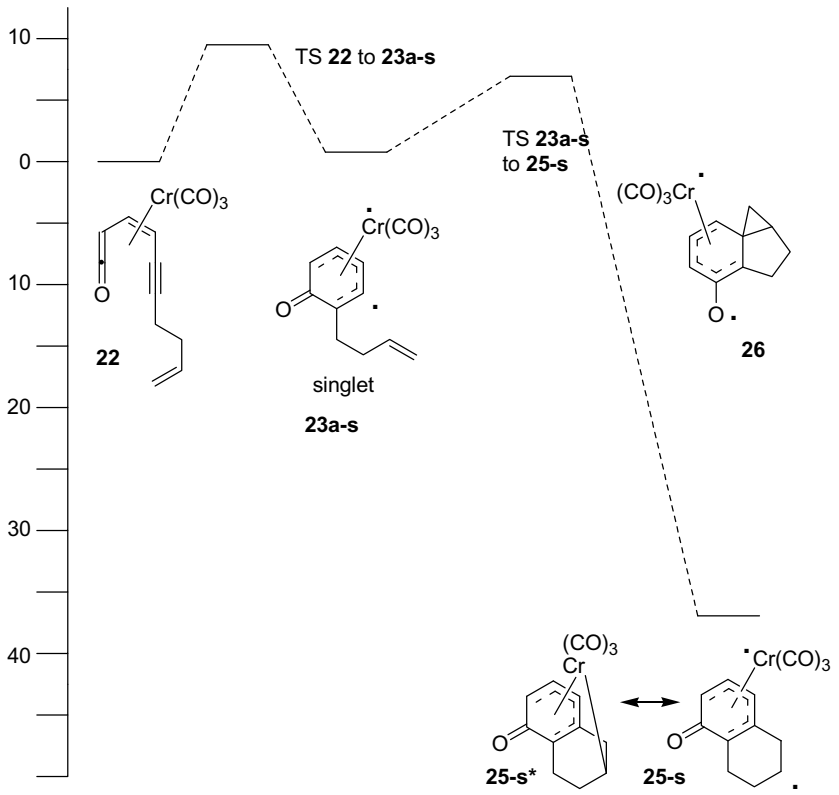

Scheme 6.

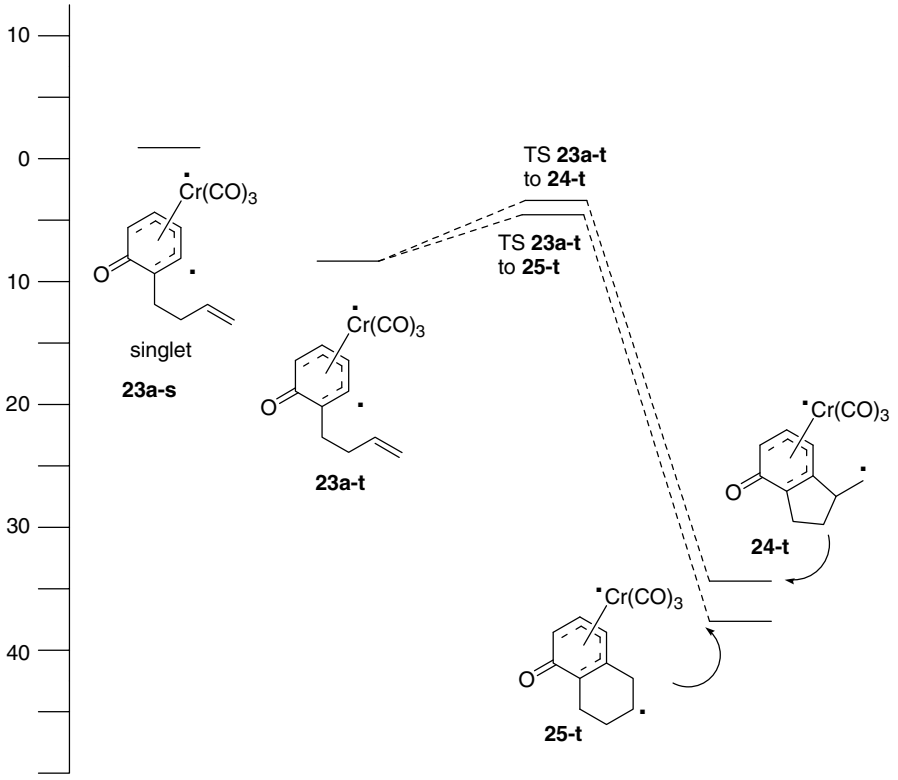

Scheme 7.

Table 3
Selected spin densities (S.D)[a] and bond lengths (Å) for intermediates **22–25**

Compound	S.D. @ Cr	S.D. @ C6	S.D. @ C10	S.D.@ C11	S.D.@ O1	C2–O1	C2–Cr	C3–Cr	C4–Cr	C5–Cr	C6–Cr	C7–Cr	C10–Cr	C11–Cr
22														
23a-s						1.22	2.69	2.36	2.30	2.18	1.89	2.26		
23a-t	1.13	0.82			0.06	1.23	2.62	2.30	2.25	2.23	2.23	2.35		
24-t	1.06			1.07	0.04	1.23	2.58	2.28	2.23	2.25	2.33	2.36		
25-s						1.23	2.65	2.35	2.27	2.23	2.18	2.27	2.43	3.20
25-t	1.02		1.02		0.05	1.23	2.55	2.29	2.27	2.25	2.29	2.33	3.99	3.44

[a] If blank, the spin density is less than 0.1.

the 5-exo- or 6-endo-derived products in a kinetically-competitive process where the 6-endo product is strongly favored thermodynamically. A limitation in all of these calculations is that the activation energy for singlet to triplet diradical interconversions can not be calculated. If the radicals freely interconvert between singlet and triplet configurations, any 5-exo-derived product **24-t** could easily convert to the 6-endo-derived product **25-s** through a pathway involving conversion to the singlet **24-s** followed by spontaneous conversion to the singlet 6-endo product **25-s**. The free energy of the triplet diradical **25-t** is very similar to that of the singlet diradicals **25-s** ($\Delta G = -1.5$ kcal/mol^{-1} for conversion of **25-s** to **25-t**) however the enthalpy is actually lower for the singlet diradicals ($\Delta H = +2.8$ kcal/mol for **25-s** to **25-t**).

3. Conclusions

In summary, the formation of arene diradicals through Moore cyclization of chromium carbene-derived enyne ketenes followed by subsequent radical cyclization reactions to pendant alkene groups has been demonstrated. The reaction proceeds predominantly through the 6-endo cyclization mode unless radical-stabilizing ester groups are positioned to stabilize the 5-exo-derived free radical intermediate. The reaction pathway was evaluated computationally using both triplet and singlet configurations of the diradicals species.

4. Experimental [28]

4.1. General procedure for the coupling of carbene complexes with diene–diynes

An 0.03–0.05 M dioxane or chlorobenzene solution of the enediyne or dienyne (1.0 eq.) and the carbene complex (1.2 eq.) was heated to 100 °C for 24 h using an oil bath heated to 100 °C. The reaction mixture was then allowed to cool to room temperature and the solvent was removed on a rotary evaporator. Hexane (15 mL) was added and the resulting green suspension was filtered through Celite. Iodine (1.5 eq.) was added to the filtrate and this solution was stirred at room temperature for 24 h. The reaction mixture was poured into aqueous sodium thiosulfate solution in a separatory funnel and the aqueous layer was extracted two times with hexane. The combined hexane layers were washed with

saturated aqueous sodium chloride solution and dried over sodium sulfate. The solvent was removed on a rotary evaporator and the crude residue was purified by chromatography on silica gel using 19:1 hexane: ethyl acetate as the eluent.

4.2. Coupling of methylcarbene complex **7a** with simple enediyne **6a** (Result in Table 1, Entry 1)

The general procedure was followed using methylcarbene complex **7a** (0.198 g, 0.7906 mmol) and dienediyne **6a** (0.112 g, 0.6588 mmol). The crude product was treated with *p*-toluenesulfonic acid monohydrate (0.0125 g, 0.06590 mmol) in dichloromethane (30 mL) for 12 h at room temperature. Purification using preparative TLC (eluent: hexanes) yielded a single fraction (0.105 g, 71% yield) which was revealed to be a 76:5:19 mixture of benzofuran-alkene **16a** (54% yield), benzofuran-alkane **13a** (3% yield), and naphthofuran **15a** (14% yield). A second preparative TLC was performed, and a pure sample of the major product, alkene **16a**, was obtained by cutting the center of the band. Benzofuran-alkene **16a**: ^{1}H NMR ($CDCl_3$): δ6.24 (s, 1H), 5.95 (br s, 2H), 3.55 (m, 2H), 3.30 (m, 2H), 2.99 (t, 2H, J = 7.3 Hz), 2.82 (t, 2H, J = 7.3 Hz), 2.43 (s, 3H), 2.15 (quintet, 2H, J = 7.3 Hz); ^{13}C NMR ($CDCl_3$): δ154.4 (quat C), 152.5 (quat C), 136.0 (quat C), 132.1 (quat C), 124.8 (quat C), 124.4 (CH), 123.6 (CH), 122.8 (quat C), 114.8 (quat C), 101.2 (CH), 31.4 (CH_2), 31.0 (CH_2), 27.4 (CH_2), 25.1 (CH_2), 23.7 (CH_2), 14.2 (CH_3); Mass Spec (El): 224 (M, 100), 223 (30), 209 (18), 196 (22), 185 (32), 182 (14), 181 (67), 179 (11), 178 (15), 167(14), 166 (17), 165 (31), 153 (11), 152 (18); HRMS calc. for $C_{16}H_{16}O$ 224.12012. Found 224.11922. Naphthofuran **15a**: ^{1}H NMR: δ8.27 (d, 1H J = 7.8 Hz), 7.85 (d, 1H J = 7.3 Hz), 7.51 (m, 2H), 6.45 (s, 1H), 3.30 (t, 2H, J = 7.4 Hz), 3.19 (t, 2H, J = 7.4 Hz), 2.59 (s, 3H), 2.34 (quintet, 2H, J = 7.4 Hz); ^{13}C NMR: δ156.5 (quat C), 150.1 (quat C), 134.0 (quat C), 133.9 (quat C), 127.7 (quat C), 125.2 (CH), 125.0 (CH), 124.6 (CH), 122.5 (quat C), 120.5 (CH), 120.4 (quat C), 102.5 (CH), 32.5 (CH_2), 31.4 (CH_2), 24.8 (CH_2), 14.5 (CH_3); MS (EI): 222 (M, 100), 207 (M−CH_3, 9), 193 (M−ethyl, 6), 179 (M−acetyl, 41); HRMS (ESI) calc. for $C_{16}H_{15}O$ (MH+) 223.1123. Found 223.1112. Spectral evidence for benzofuran-alkane **13a**: ^{1}H NMR ($CDCl_3$): The crude ^{1}H NMR spectrum features peak at δ 1.23 (d, J = 6.9) which is consistent with the nonallylic methyl of **14a**; GCMS (EI): 226 (M, 34), 211 (M−CH_3, 100), 198 (M−ethylene, 3), 183 (M−acetyl, 16).

4.3. Coupling of methylcarbene complex **7a** with ethylidene enediyne **6b** in dioxane (Result in Table 1, Entry 2)

The general procedure was followed using methylcarbene complex **7a** (0.458 g, 1.833 mmol) and dienediyne **6b** (0.270 g, 1.466 mmol) and using dioxane (30 mL) as solvent. Final purification using flash column chromatography (silica gel/9:1 hexanes: ethyl acetate) yielded a single fraction (0.185 g, 53% yield) identified as a 3:1 mixture of benzofuran **16b** (40% yield) and naphthofuran **15b** (13% yield). Further purification by preparative TLC and cutting the slowest one third of the band yielded pure **16b**. Naphthofuran **15b** could not be obtained free of benzofuran **16b**. Benzofuran **16b**: ^{1}H NMR ($CDCl_3$): δ6.26 (s, lH), 5.97 (m, 2H), 3.60–3.35 (m, 3H), 2.99 (t, 2H, J = 8.0 Hz), 2.91 (t, 2H, J = 8.0 Hz), 2.43 (s, 3H), 2.12 (quintet, 2H, J = 8.0 Hz), 1.22 (d, 3H, J = 6.0 Hz); ^{13}C NMR ($CDCl_3$): δ154.6, 150.1, 135.5, 132.9, 131.9, 131.2, 122.6, 115.0, 101.2, 32.3, 31.3, 31.2, 25.5, 23.8, 22.4, 14.2; IR (neat): 3025, 2943, 2841, 1594, 1427 cm^{-1}; MS (EI): 238 (M, 50), 223 (100), 211 (18), 195 (21); HRMS: Calc. for $C_{17}H_{18}O$ 238.1358. Found 238.1370. Naphthofuran **15b** (mixture with **16b** – peaks for **16b** omitted): ^{1}H NMR ($CDCl_3$): δ8.12 (d, 1H, J = 8.0 Hz), 7.32 (t, 1H, J = 8.0 Hz), 7.19 (d, 1H, J = 8.0 Hz), 6.40 (q, 1H, J = 1.0 Hz), 3.09 (t, 2H, J = 7.7 Hz), 2.96 (t, 2H, J = 7.7 Hz), 2.88 (s, 3H), 2.55 (d, 3H, J = 1.0 Hz), 2.23 (quintet, 2H, J = 7.7 Hz); ^{13}C NMR ($CDCl_3$): δ154.5, 152.3, 135.3, 134.6, 133.4, 132.9, 128.1, 127.4, 124.5, 118.8, 102.1, 36.3, 31.5, 25.1, 24.5, 14.3.

4.4. Coupling of methylcarbene complex **7a** with ethylidene enediyne **6b** in chlorobenzene (Result in Table 1, Entry 3)

The general procedure was followed using methylcarbene complex **7a** (0.458 g, 1.833 mmol) and dienediyne **6b** (0.270 g, 1.466 mmol) and using chlorobenzene (30 mL) as solvent. Final purification using flash column chromatography (silica gel/9:1 hexanes: ethyl acetate) yielded a single fraction (0.170 g, 49% yield) that revealed to be a 9:1 mixture of compounds **16b** (45% yield) and **15b** (4% yield). The spectral data were identical to the same products obtained in dioxane (previous experiment).

4.5. Coupling of phenylcarbene complex **7b** with ethylidene enediyne **6b** in chlorobenzene (Result in Table 1, Entry 4)

The General Procedure was followed using phenylcarbene complex **7b** (0.622 g, 1.994 mmol) and dienediyne **6b** (0.306 g, 1.661 mmol) and using chlorobenzene (30 mL) as solvent. Final purification using flash column chromatography (silica gel/9:1 hexanes:ethyl acetate) yielded a single fraction (0.233 g, 47% yield) identified as a 19:1 mixture of benzofuran **16c** (45% yield) and naphthofuran **15c** (2% yield). Further purification by preparative TLC yielded benzofuran **16c** free of naphthofuran **15c**. Benzofuran **16c**: ^{1}H NMR ($CDCl_3$): δ7.85 (d, 2H, J = 8.0 Hz), 7.38 (m, 3H), 6.93 (s, 1H), 6.00 (br s, 2H), 3.74 (m, 1H), 3.49 (m, 2H), 3.06 (t, 2H, J = 8.0 Hz), 2.94 (t, 2H, J = 8.0 Hz), 2.18 (m, 2H), 1.26 (d, 3H, J = 7.0 Hz); ^{13}C NMR ($CDCl_3$): δ156.3, 152.5, 135.9, 132.6, 131.8, 131.0, 128.6, 128.0, 128.5, 126.9, 124.6, 122.6, 115.5, 100.0, 32.4, 31.2, 29.7, 25.5, 23.8, 22.3; Mass Spec (El): 300 (M, 83), 298 (18), 286 (25), 285 (100), 257 (30), 229 (18), 154 (21), 105 (15), 91(13); HRMS calc. for $C_{22}H_{20}O$ 300.1529. Found 300.1514. For **15c** spectral data, see the next experiment.

4.6. Coupling of phenylcarbene complex **7b** with ethylidene enediyne **6b** in benzene solvent (Result in Table 1, Entry 5)

The General Procedure was followed using phenylcarbene complex **7b** (0.563 g, 1.805 mmol) and dienediyne **6b** (0.277 g, 1.504 mmol) and using benzene (30 mL) as solvent. The reaction was conducted at the reflux temperature of benzene. Final purification using flash column chromatography (silica gel/20:1 hexanes:ethyl acetate) yielded compound **15c** (0.091 g, 21% yield). Compound **15c**: ^{1}H NMR ($CDCl_3$): δ8.28 (d, 1H, J = 8.0 Hz), 7.96 (d, 2H, J = 8.0 Hz), 7.39 (m, 4H), 7.07 (s, 1H), 3.66 (t, 2H, J = 8.0 Hz), 3.18 (t, 2H, J = 8.0 Hz), 2.91 (s, 3 H), 2.27 (quintet, 2H, J = 8.0 Hz); ^{13}C NMR ($CDCl_3$): δ157.0, 155.4, 137.2, 136.6, 135.9, 134.9, 133.1, 131.1, 129.8, 128.9, 128.2, 124.7, 119.3, 101.1, 36.4, 31.6, 25.0, 24.5; UV: λ_{MAX} = 242, 262, 284, 294, 314, 328, 348, 364 (nm) Mass Spec (El): 298 (M, 23), 105 (100), 91(37), 76 (46), 51(13); HRMS calc. for $C_{22}H_{18}O$ 298.1358. Found 298.1364.

4.7. Coupling of carbene complex **7a** with dienediyne methyl ester **6c** (Result in Table 1, Entry 6)

The General Procedure was followed using methylcarbene complex **7a** (0.307 g, 1.227 mmol) and dienediyne **6c** (0.214 g, 0.982 mmol) and using dioxane (22.5 mL) as solvent. Final purification using flash column chromatography (silica gel/4:1 hexanes:ethyl acetate) yielded compound **14d** (0.133 g, 48% yield). ^{1}H NMR ($CDCl_3$): δ6.27 (s, 1H), 3.70 (s, 3H), 3.70 (m, 1H, linewidth = 19.1 Hz), 3.20–2.70 (m, 8H), 2.43 (s, 3H), 2.40 (dt, 2H, J = 13.0, 5.0 Hz), 2.18 (quintet, 2H, J = 8.0 Hz); ^{13}C NMR ($CDCl_3$):

δ173.4, 154.9, 152.2, 137.3, 134.1, 133.3, 124.6, 122.8, 101.3, 51.5, 41.1, 38.6, 31.7, 30.7, 30.2, 26.9, 25.7, 14.0; IR (neat): 2948 (s), 2847 (m), 1739 (s), 1435 (m), 1213 (s), 1158 (s) cm^{-1}; MS (EI): 284 (M, 30), 211 (100); HRMS: Calc. for $C_{18}H_{20}O_3$ 284.1412. Found 284.1414.

Acknowledgements

This research was supported by the Petroleum Research Fund, Administered by the American Chemical Society (JWH), the SCORE program of NIH (S06 GM008136) (JWH), and National Science Foundation CAREER award CHE-0348956 (HW). We are grateful to a reviewer for insightful comments.

Appendix A. Supplementary material

General experimental and synthetic procedures for the preparation of diene–diynes **6a–c** and copies of ^1H NMR and ^{13}C NMR spectra for compounds **6a–c**, **14d**, **15a, 15c**, **16a–c**. Atomic coordinates, energies, and spin densities for all of the energy-minimized structures in Fig. 1 plus relevant transition states. Supplementary data associated with this article can be found, in the online version, at doi:10.1016/j.jorganchem.2008.08.003.

References

[1] For a recent review, see; U. Galm, M.H. Hager, S.G. Van Lanen, J. Ju, J.S. Thorson, B. Shen, Chem. Rev. 105 (2005) 739–758.
[2] (a) Recent Examples; M. Zora, M. Kokturk, T. Eralp, Tetrahedron 62 (2006) 10344–10351;
(b) J.E. Ezcurra, K. Karabelas, H.W. Moore, Tetrahedron 61 (2005) 275–286;
(c) P. Wipf, C.R. Hopkins, J. Org. Chem. 64 (1999) 6881–6887;
(d) Y. Xiong, H. Xia, H.W. Moore, J. Org. Chem. 60 (1995) 6460–6467;
(e) L.M. Gayo, M.P. Winters, H.W. Moore, J. Org. Chem. 57 (1992) 6896–6899.
[3] A. Padwa, U. Chiacchio, D.J. Fairfax, J.M. Kassir, A. Litrico, M.A. Semones, S.L. Xu, J. Org. Chem. 58 (1993) 6429–6437.
[4] N.V. Nguyen, K. Chow, J.O. Karlsson, R.J. Doedens, H.W. Moore, J. Org. Chem. 51 (1986) 419–420.
[5] A. Tarli, K.K. Wang, J. Org. Chem. 62 (1997) 8841–8847.
[6] J.W. Grissom, G.U. Gunawardena, D. Klingberg, D. Huang, Tetrahedron 52 (1996) 6453–6518.
[7] For a recurring annual series on the reactivity of carbene complexes, see; J.W. Herndon, Coord. Chem. Rev. 251 (2007) 1158–1258. earlier editions of the series.
[8] For a preliminary account of this work, see; J.W. Herndon, H. Wang, J. Org. Chem. 63 (1998) 4562–4563.
[9] A. Rahm, W.D. Wulff, J. Am. Chem. Soc. 118 (1996) 1807–1808.
[10] K.K. Wang, B. Liu, Y. Lu, Tetrahedron Lett. 36 (1995) 3785–3788.
[11] The incorrect assignment was based on accidental isochrony attributed to the two alkene protons of **13a**, coupled with a preponderance of evidence that suggests radical cyclizations favor 5-exo processes over 6-endo processes. See: Curran, D.P. Synthesis 1988, 417–439 and Synthesis 1988, 489–513.
[12] For oxidative dehydrogenation by chromium(0) species, see; S.U. Tumer, J.W. Herndon, L.A. McMullen, J. Am. Chem. Soc. 114 (1992) 8394–8404.
[13] M.E. Bos, W.D. Wulff, R.A. Miller, S. Chamberlin, T.A. Brandvold, J. Am. Chem. Soc. 113 (1991) 9293–9319.
[14] (a) For recent examples M.A. Grundl, D. Trauner, Org. Lett. 8 (2006) 23–25;
(b) M.C. Elliott, N.N.E. El Sayed, Tetrahedron Lett. 46 (2005) 2957–2959;
(c) N. Kurono, E. Honda, F. Komatsu, K. Orito, M. Tokuda, Tetrahedron 60 (2004) 1791–1801;
H. Ishibashi, T. Kobayashi, D. Takamasu, Synlett (1999) 1286–1288.
[15] E.P. Kündig, H. Ratni, B. Crousse, G. Bernardinelli, J. Org. Chem. 66 (2001) 1852–1860.
[16] Y. Zhang, J.W. Herndon, Tetrahedron 56 (2000) 2175–2184.
[17] J.W. Grissom, D. Klingberg, D. Huang, B.J. Slattery, J. Org. Chem. 62 (1997) 603–626.
[18] A.N. Abeywickrema, A.L.J. Beckwith, S. Gerba, J. Org. Chem. 52 (1987) 4072–4078.
[19] For a review of arene–$Cr(CO)_3$ complexes see; M. Uemura, Org. React. 67 (2006) 217–657.
[20] C.A. Merlic, Bruce N. Hietbrink, K.N. Houk, J. Org. Chem. 66 (2001) 6738–6744.
[21] Frisch, M.J. et al, GAUSSIAN 03, revision C.02; Gaussian, Inc.: Wallingford, CT, 2004.
[22] A.D. Becke, J. Chem. Phys. 98 (1993) 5648.
[23] C. Lee, W. Yang, R.G. Parr, Phys. Rev. B 37 (1988) 785.
[24] (a) M. Dolg, U. Wedig, H. Stoll, H. Preuss, J. Chem. Phys. 86 (1987) 866;
(b) D. Andrae, U. Haussermann, M. Dolg, H. Stoll, H. Preuss, Theor. Chim. Acta 77 (1990) 123.
[25] The value for the C–O bond in the simple ketone benzophenone is 1.23 Å; E.B. Fleischer, N. Sung, S. Hawkinson, J. Phys. Chem. 72 (1968) 4311–4312.
[26] (a) V.W. Manner, T.F. Markle, J.H. Freudenthal, J.P. Roth, J.M. Mayer, Chem. Commun. (2008) 256–258;
(b) D.E. Williams, Mol. Phys. 16 (1969) 145–151.
[27] (a) L. Weber, D. Wewers, R. Broese, Chem. Ber. 118 (1985) 3570–3578;
(b) P.G. Cozzi, P. Veya, C. Floriani, F.P. Rotzinger, A. Chiesi-Villa, C. Rizzoli, Organometallics 14 (1995) 4092–4100;
(c) H.G. Raubenheimer, M.W. Esterhuysen, G. Frenking, A.Y. Timoshkin, C. Esterhuysen, U.E.I. Horvath, Dalton Trans. (2006) 4580–4589.
[28] For a General Experimental, see the Supplementary Material.